



# Low-cost GNSS antennas in precise positioning: a focus on multipath and antenna phase center models

Grzegorz Krzan<sup>1</sup> · Karol Dawidowicz<sup>1</sup> · Jacek Paziewski<sup>1</sup>

Received: 4 September 2023 / Accepted: 22 March 2024  
© The Author(s) 2024

## Abstract

The rapid growth of the GNSS equipment market has put affordable receivers and antennas capable of receiving satellite signals into the hands of users. High positioning accuracy, previously achievable only with high-grade devices, is becoming possible with low-cost ones. However, simplifications in the design of these devices, intended to reduce the manufacturing cost, affect their capabilities. This study analyzes the positioning accuracy that may be achieved with recent low-cost antennas. We put particular stress on investigating the susceptibility of such antennas to the multipath effect and implications from the quality of the antenna phase center models. The positioning performance is assessed by employing the Precise Point Positioning method with the integer ambiguity resolution of phase observations. The results obtained with three low-cost antennas are validated against three high-grade antennas. We reveal a two- to threefold decrease in positioning performance with low-cost antennas compared to high-quality equipment. However, positioning accuracy increased when a low-cost antenna with a phase correction model was used, particularly for the eastern component of coordinate bias. In addition, a significant susceptibility of low-cost antennas to the multipath effect was confirmed, especially for GPS L2 and Galileo E5a signals.

**Keywords** PPP-AR · Low-cost GNSS antennas · Multipath · Phase center corrections

## Introduction

In recent years, numerous low-cost devices have appeared on the market, with their capabilities gradually approaching that of high-grade ones. As a result, low-cost antennas and receivers become the object of interest for those who demand high precision and reliability of positioning at an affordable price. Many surveying applications, such as deformation monitoring, require continuously operating networks of antennas and receivers. The cost of establishing such networks can be reduced when using low-cost antennas (Hohensinn et al. 2022).

However, the low manufacturing cost of the devices also comes with compromises in their design, limited capabilities, or susceptibility to error sources. In the case of low-cost antennas, we can identify two main error sources critical for precise GNSS positioning: phase center variation (PCV) of the receiving antenna and multipath (MP). MP can be treated

as a source of time-dependent errors due to the changing but repeatable within a single navigation system configuration of satellites in the sky. On the other hand, phase center characteristics are independent of the antenna location. Nevertheless, both will depend on the azimuth and elevation angle of the satellites. Since PCV and MP are independent errors, their careful separation is necessary for accurate correction and modeling.

In static positioning, it is commonly assumed that the impact of the multipath effect fully averages during long observation sessions. This assumption, unfortunately, is valid only in the case of short periodic multipath signals caused by distant objects located in the far-field region of the antenna (Volk and Levine 1994). The signal reflections from the closest vicinity of the antenna introduce long periodic errors, which are nonzero mean distributed, and therefore introduce a bias in the estimated parameters. This is especially true for ascending and descending satellites tracked at low elevation angles. Additionally, reflecting objects in the antenna's near-field region can change the overall electromagnetic properties of the antenna (Dilßner et al. 2008).

Over the years of multipath research, in addition to defining measurement principles that reduce its impact, two main

✉ Grzegorz Krzan  
grzegorz.krzan@uwm.edu.pl

<sup>1</sup> University of Warmia and Mazury in Olsztyn, Ul. Oczapowskiego 2, 10-720 Olsztyn, Poland

methods of mitigating this phenomenon have been developed: baseband signal processing technology and antenna-based technology. Various scientific teams have developed the former methods for more than two decades (Ge et al. 2000; Bhuiyan and Lohan 2010; Rougerie et al. 2012). However, as this study focuses on antenna-based technology, they will not be discussed in detail in this work.

Using choke-ring-ground-plane antennas, antenna arrays, and antennas with strong right-hand circular polarization sensitivity is one strategy leveraging antenna-based mitigation strategies. A significant left-hand circular polarization component is generally present in the reflected signals (Parkinson and Spilker 1996). The use of an Eccosorb AN-W-79 microwave-absorbing material fitted around a GNSS antenna that reflects less than 17 dB of typical incident radiation above a frequency of 600 MHz has recently been proposed by Hunegnaw and Teferle (2022). The above techniques apply to professional antennas. Hamza et al. (2021) state that low-cost antennas are more susceptible to multipath.

Another critical issue of precise GNSS positioning in the context of antennas is the application of precise phase center corrections (PCC). Changes in the position of the antenna phase center can have an amplitude of up to several centimeters. Neglecting them can lead to serious biases in both the vertical and horizontal components of the coordinates. It is necessary to perform calibration to determine such characteristics of the antenna. The most commonly employed methods are absolute calibration in the field using a robot or calibration in an anechoic chamber (Wübbena et al. 2006; Görres et al. 2006). Unfortunately, unlike professional ones, most low-cost antennas do not have such calibrations. Thus, the antenna phase patterns are poorly defined, which consequently degrades positioning accuracy. Recent studies have shown noticeable PCV values of up to 2 cm at L1 and 4 cm at L5 for low-cost antennas obtained by absolute calibration (Darugna et al. 2020). These results show that knowledge of PCV of low-cost antennas is essential to improve their performance.

Many studies on applying low-cost antennas considered relative positioning under favorable observation conditions. In this regard, Biagi et al. (2016) test the U-blox receiver and low-cost antenna for landslide monitoring. Relative positioning mode over a short baseline allowed them to achieve positioning accuracy with a standard deviation (STD) of 5 mm horizontally and 5 to 13 mm vertically. However, Jackson et al. (2018) point out that positioning accuracy is greatly affected by the environment of the measurement point. Similar conclusions were reached by Garrido-Carretero et al. (2019), who reported that positioning accuracy decreases sharply with baseline extension. Multi-frequency low-cost GNSS receivers were also tested in combination with geodetic and low-cost antennas (Guerova et al. 2016; Xue et al. 2021), this time paying particular attention to the need

to calibrate antennas to achieve high-quality positioning results. More recently, Paziewski (2022) revealed a meaningful drop in the performance of single-frequency Precise Point Positioning (PPP) with low-cost antennas compared to the solution based on high-quality equipment and attributed such results to the susceptibility to the multipath effect.

As the ionospheric-free (IF) linear combination commonly employed in PPP amplifies the PCC values almost threefold compared to the uncombined L1 and L2 signals, the quality of correction models for low-cost antennas becomes a crucial issue to be handled in such a case. Moreover, the existing studies on low-cost antennas mainly deal with relative positioning without thoroughly exploring the implications of the multipath effect. Therefore, motivated by user demands and the limitations of existing literature in the field, we assess the performance of multi-GNSS PPP with low-cost antennas, focusing on the impacts of antenna correction models and multipath susceptibility. In this regard, we employ selected recent low-cost antennas with and without calibrations.

In the next section, we describe the experiment design, i.e., the antenna models used in the study, data collection, and processing methods. The following section is devoted to discussing the experiment results in terms of positioning accuracy, ambiguity fixing rate, and multipath values. Finally, in the last section, we summarize and disseminate the results.

## Experiment design

We verify the applicability of low-cost GNSS antennas to precise geodetic applications by assessing positioning performance based on GNSS data collected using representative antennas. We use PPP mode, whose current accuracy allows it to be placed on par with the relative method. We use positioning indicators, which are typically adopted for precise positioning with high-grade equipment.

### Specification of the employed GNSS antennas

A set of three antennas, such as U-blox ANN-MB-00, Tallysman TW7972, and ELT0149, supporting quad constellations was proposed to analyze the feasibility of using low-cost GNSS antennas for precision geodetic applications. In addition, two surveying-grade antennas and one geodetic choke-ring antenna were employed to provide benchmark solutions (Table 1, Fig. 1).

In the case of low-cost antennas, the specifications given by manufacturers state some differences in the signals they register. However, analysis of recorded observations indicates that all antennas recorded the same signals,

i.e., GPS L1/L2/L5, GLONASS G1/G2/G3, Galileo E1/E5a/E5b/E6, and Beidou B1/B2a/B2b/B1-2/B3. We have analyzed the number of observations recorded by each antenna in the further part of the study. The antennas are also characterized by different information on antenna phase center offset and variations. For the ELT0149, there is no information on both phase center offset and variation. For U-blox ANN-MB-00, the only available information is up PCO for GPS L1 and L2 signals. The Tallysman TW7972 antenna is the only one among the tested that has almost complete information regarding PCC. However, these corrections came from relative calibration and were then converted to values compatible with the results of absolute calibration. Moreover, the corrections are given only as a function of the zenith angle. A lack of corrections as a function of the azimuth of the incoming signal may adversely affect the accuracy of the solution. Another drawback is a lack of corrections for other GNSS signals. Last but not least, the ANN-MB-00 antenna has a defined radiation pattern in L1 and L2 band. It describes a high

low-noise amplifier gain (28 dB) for signals coming from directions near the zenith and a much lower one for signals coming from horizontal directions (> 20 dB) to the nadir (negative dB values). Such antenna characteristics support the antenna’s robustness to the multipath effect; however, it does not completely eliminate the reception of signals coming from negative elevation angles, most of which are reflected signals. For the TW7972 and ELT0149 antennas, the manufacturers do not provide detailed radiation pattern characteristics, however, specifying a typical gain for signals coming from the zenith of 32 dB and 38 dB, respectively. Detailed specifications for the antennas can be found in the antenna manufacturers’ datasheets.

If we compare only the PCO, it can be seen, as expected, that the biggest differences occurred in the case of the Up component (Table 1). For GPS L1 frequency, L1 PCO range from 8.90 mm (U-blox ANN-MB-00 antenna) to 114.07 mm (TRM159900.00 NONE antenna). In the case of GPS L2 PCO, differences are even higher, ranging from 7.60 mm to 123.95 mm for the same two antennas. The

**Table 1** Antennas used in the study and their PCO for GPS signals

Antenna model	Serial no	GPS L1 PCO [mm]			GPS L2 PCO [mm]		
		N	E	U	N	E	U
TRM159900.00 NONE	6126333759	0.61	0.08	114.07	0.25	0.52	123.95
TRM105000.10 NONE #1	3121102632	0.43	0.00	61.66	-0.47	2.66	56.54
TRM105000.10 NONE #2	61053R0021	0.43	0.00	61.66	-0.47	2.66	56.54
U-blox ANN-MB-00 #1	AGA556022-S0-A24	-	-	8.90	-	-	7.60
U-blox ANN-MB-00 #2	AGA556022-S0-A9	-	-	8.90	-	-	7.60
Tallysman TW7972 #1	20210910	0.86	-1.13	10.34	-0.59	2.34	9.95
Tallysman TW7972 #2	20210630	0.86	-1.13	10.34	-0.59	2.34	9.85
ETL0149	-	-	-	-	-	-	-
JAVGRANT-G3T NONE	01348	1.22	0.42	50.28	-3.17	1.22	46.83

**Fig. 1** GNSS antennas used in the experiment. The top row shows low-cost antennas ELT0149 (left), U-blox ANN-MB-00 (middle), and Tallysman TW7972 (right). High-grade antennas are given in the bottom row: JAVGRANT-G3T (left), TRM105000.10 (middle), and TRM159900.00 (right)



high-grade antennas used in the study, i.e., TRM159900.00, TRM105000.10, and JAVGRANT-G3T, have complete phase center position information for GPS and GLONASS signals obtained from absolute calibrations (Fig. 2). Analyzing data presented in Fig. 2, it is visible that the smallest PCV values, not exceeding 3 mm, are revealed for the TRM105000.10 antenna. On the other hand, the largest spread of PCV values, from  $-6$  to  $12$  mm, is seen in the case of the TRM159900.00. It should be noted that all the PCO/PCV values given are from type-mean models, which are usually values averaged from calibrating several units of a specific antenna model. For geodetic antennas, one can also find individual PCC models from field robot or anechoic chamber calibrations, determined for a specific antenna unit.

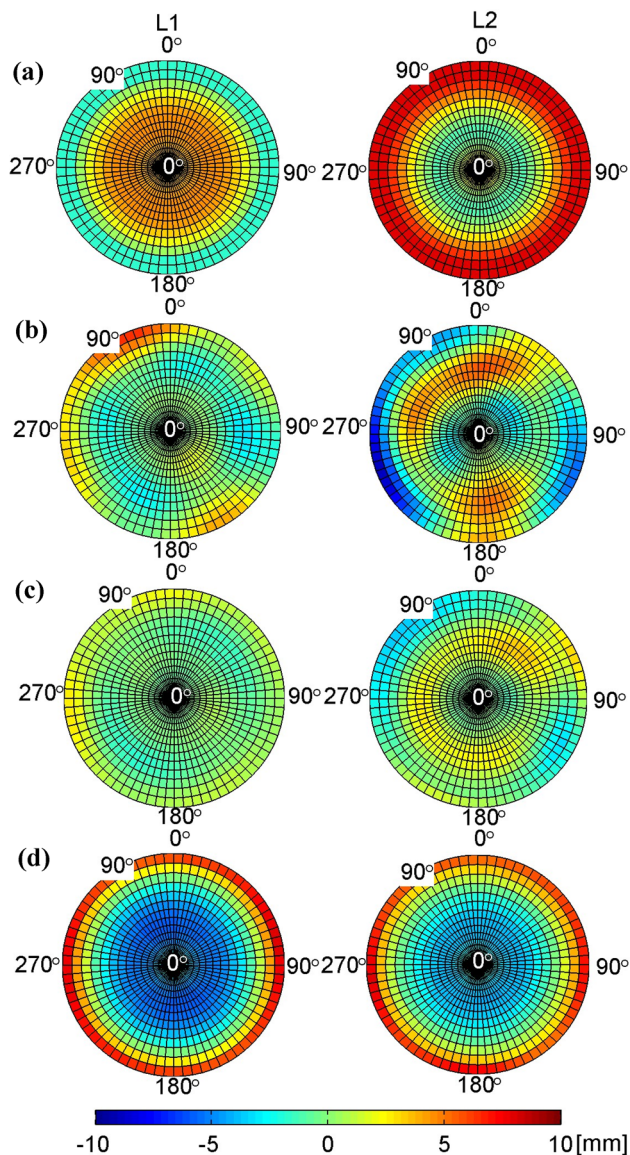


**Fig. 2** Antenna PCV patterns: a) Tallysman TW7972, (b) JAVGRANT-G3T, c) TRM105000.10, d) TRM159900.00

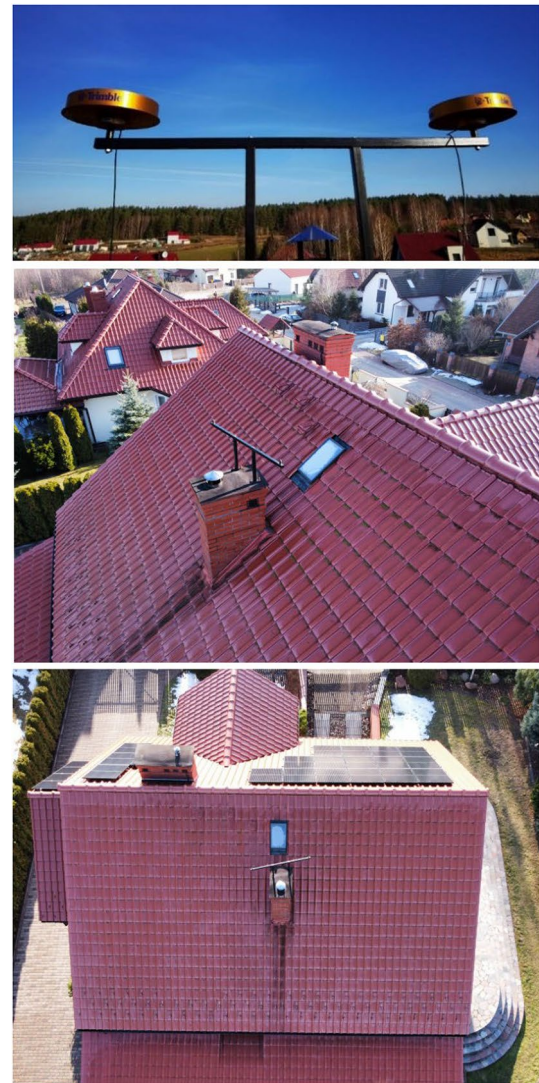


**Fig. 3** Mounting the antennas on the test beam and its surroundings

## Data collection

In the study, we used two units of TRM105000.10, Tallysman TW7972, U-blox ANN-MB-00 antenna models, and single units of ELT0149 and TRM159900.00 NONE. Each tested antenna was connected to the Trimble Alloy receivers. The antennas were collocated during the experiment as they were placed on a rigid beam with two antenna mounting points. The beam was placed on the roof of a residential building (Fig. 3). The distance between the antenna mounting points was determined with a high accuracy of  $0.5$  mm and reached  $1601.0$  mm. The beam was also precisely leveled with an error of  $0.3$  mm to ensure that the two antennas were of equal height. Since identical receivers with the same configurations and cabling were used, the observation conditions can be considered the same for the two antennas

being compared. Any differences in results may indicate differences in signal tracking quality caused by antennas. The location of the test beam on a chimney located on a sloping roof with a wavy ceramic covering will more than likely be a source of reflected signals related to multipath. GNSS data were collected for over 13 days. The observation time for each day was 16 h, from 8 a.m. to 24 a.m. GPS time. An interval of 5 s and an elevation mask of  $0^\circ$  were adopted for the data collection. Table 2 summarizes the configuration of the antennas on the measuring beam for each day.

We analyzed the number of observations recorded at the measurement points on each day in Table 3. For simplicity, we report only the number of carrier phase observations, since the number of code observations did not differ by more than 1% and show only signals used in the later processing. It can be seen that the differences between the number of recorded observations when the same antennas were on mounting points 1 and 2 in almost all cases do not exceed 2%. The exception is Beidou signals, when low-cost antennas were operating on both points—then the difference reached 6–9%. Similar differences also occurred when different antennas worked on the points. The reason is most likely that the Beidou B1–2 and B3 signals associated with L2I and L6I carrier phases are not listed as supported by the low-cost antenna as well as JAVGRANT-G3T specifications. For GPS signals for each pair of antennas, the differences in the number of recorded observations did not exceed 2%. For the other systems, noticeable differences can be seen when the TRM159900.00 antenna was operating on one of the points. The choke-ring design of this antenna, which is meant to filter reflected signals from low elevation angles, probably resulted in fewer observations recorded.

## Positioning method

The GNSS data were processed in static and kinematic PPP mode with phase ambiguity resolution (PPP-AR), using PRIDE PPP-AR 2.2 software. The PPP method is based on the ionospheric-free linear combination (IF) that eliminates the first order of ionospheric delay which accounts for 99.9% of this effect. However, a well-known consequence of using the IF linear combination is that we may expect the noise of combined observables to be a factor of three with respect to original observations (Paziewski et al. 2019). Also, an increase in MP is observed when linear combinations of observations are created (Moradi 2014). To resolve wide-lane and narrow-lane ambiguities, Hatch–Melbourne–Wübbena linear combination is used. Detailed information on the algorithms used by PRIDE PPP-AR can be found in the program’s documentation (Geng et al. 2019).

We investigate the result of the static solution derived from a processing of 16-h long dataset for each day of data collection and the coordinate time series obtained in a kinematic solution with an interval of 5 s. The processing was performed in two variants: using GPS-only (G) or multi-constellation observations from GPS, GLONASS, Galileo, and BDS (GREC). We utilized the type-mean PCCs included in the IGS14\_2196.atx file for professional surveying antennas used as benchmarks. For the Tallysman TW7972 antenna, the PCCs provided by the manufacturer were used, as well as PCO for U-blox ANN-MB-00. For ELT0149, zero PCCs were assumed, as no correction models are available. Detailed parameters of the processing strategy can be found in Table 4.

**Table 2** Antenna configuration during data collection

Date	Antenna	
	Mounting point #1	Mounting point #2
18.03.2022 (DOY 077)	U-blox ANN-MB-00 #1	U-blox ANN-MB-00 #2
19.03.2022 (DOY 078)	TRM105000.10 NONE #1	TRM105000.10 NONE #2
20.03.2022 (DOY 079)	U-blox ANN-MB-00 #2	ELT0149
21.03.2022 (DOY 080)	U-blox ANN-MB-00 #2	TRM159900.00 NONE
22.03.2022 (DOY 081)	U-blox ANN-MB-00 #1	TRM159900.00 NONE
23.03.2022 (DOY 082)	TRM105000.10 NONE #2	TRM159900.00 NONE
24.03.2022 (DOY 083)	U-blox ANN-MB-00 #2	JAVGRANT-G3T NONE
25.03.2022 (DOY 084)	U-blox ANN-MB-00 #1	JAVGRANT-G3T NONE
26.03.2022 (DOY 085)	Tallysman TW7972 #1	JAVGRANT-G3T NONE
27.03.2022 (DOY 086)	Tallysman TW7972 #1	ELT0149
28.03.2022 (DOY 087)	Tallysman TW7972 #1	TRM159900.00 NONE
29.03.2022 (DOY 088)	Tallysman TW7972 #1	Tallysman TW7972 #2
30.03.2022 (DOY 089)	Tallysman TW7972 #1	U-blox ANN-MB-00 #2

**Table 3** Differences in the number of recorded carrier phase observations on mounting points 1 and 2. Positive values indicate that more observations were recorded on point 1

DOY	Mounting point #1	Mounting point #2	GPS		GLONASS		Galileo		Beidou	
			L1C	L2X	L1P	L2C	L1X	L5X	L2I	L6I
077	U-blox ANN-MB-00 #1	U-blox ANN-MB-00 #2	-1%	-1%	-2%	-1%	2%	-2%	6%	9%
078	TRM105000.10 NONE #1	TRM105000.10 NONE #2	0%	0%	-1%	-1%	0%	0%	1%	2%
079	U-blox ANN-MB-00 #2	ELT0149	-1%	-1%	6%	4%	0%	4%	-3%	-3%
080	U-blox ANN-MB-00 #2	TRM159900.00 NONE	2%	1%	4%	2%	13%	11%	6%	-3%
081	U-blox ANN-MB-00 #1	TRM159900.00 NONE	2%	0%	4%	0%	11%	8%	8%	-8%
082	TRM105000.10 NONE #2	TRM159900.00 NONE	2%	2%	7%	6%	11%	10%	9%	10%
083	U-blox ANN-MB-00 #2	JAVGRANT-G3T NONE	-1%	-2%	-1%	-7%	1%	-2%	2%	-18%
084	U-blox ANN-MB-00 #1	JAVGRANT-G3T NONE	-1%	-1%	0%	-4%	0%	-2%	2%	-18%
085	Tallysman TW7972 #1	JAVGRANT-G3T NONE	0%	-1%	1%	-1%	0%	-2%	4%	-18%
086	Tallysman TW7972 #1	ELT0149	0%	1%	1%	2%	2%	6%	7%	-9%
087	Tallysman TW7972 #1	TRM159900.00 NONE	2%	2%	5%	4%	14%	11%	10%	-7%
088	Tallysman TW7972 #1	Tallysman TW7972 #2	0%	0%	-1%	1%	2%	2%	2%	-6%
089	Tallysman TW7972 #1	U-blox ANN-MB-00 #2	0%	1%	0%	1%	2%	2%	7%	1%

### Methods for multipath study

The susceptibility of antennas to the MP effect for GPS L1 and L2, as well as Galileo E1 and E5a signals, was investigated by taking advantage of the Code-Minus-Carrier (CMC) linear combination of GNSS signals. For GPS signals, code MP error was derived as follows (Vázquez et al. 2012):

$$MP_1 = P_1 - \left(1 + \frac{2}{\alpha - 1}\right)\Phi_1 + \left(\frac{2}{\alpha - 1}\right)\Phi_2 \tag{1}$$

$$MP_2 = P_2 - \left(\frac{2\alpha}{\alpha - 1}\right)\Phi_1 + \left(\frac{2\alpha}{\alpha - 1} - 1\right)\Phi_2 \tag{2}$$

where  $P_1$  and  $P_2$  are pseudorange measurements on L1 and L2 frequencies,  $\Phi_1$  and  $\Phi_2$  are carrier phase measurements on L1 and L2 frequencies,  $\alpha = \left(\frac{f_1}{f_2}\right)^2$ ,  $f_1$  frequency of L1,  $f_2$  frequency of L2. The CMC formulas in the case of Galileo signals were derived correspondingly.

**Table 4** Processing parameters

Parameter	Setting
GNSS constellations	G or GREC
Observations	IF linear combination of dual-frequency signals from quad constellations
Stochastic modeling	a priori noise of pseudorange and phase: 0.30 m and 0.01 cycle
Solution type	PPP with ambiguity resolution, static (16 h) and kinematic (5 s interval)
Elevation angle	10°
Orbits, clocks, earth rotation parameters	Wuhan University rapid products (WUM) (Guo et al. 2016)
Differential code bias (DCB)	WUM
PCC model	IGS14_2196 for geodetic-grade antennas (type-mean), Tallysman TW7971 PCC model (type-mean) U-blox ANN-MB-00 PCO (type-mean) Zero PCC for ELT0149
Ocean loading model	FES2004
Tidal displacements	IERS Conventions 2010
Troposphere delay handling	Saastamoinen model with Global Pressure and Temperature (GPT) and Global Mapping Function (GMF) estimated every hour; priori constraint of ZTD and process noise: 0.20 m
Horizontal troposphere gradient handling	Estimated every 2 h (piece-wise constant); priori constraint of HTG: 0.005 m
Ionospheric delay handling	First order eliminated with IF linear combination, higher orders neglected
Ambiguity resolution method	Wide-lane/narrow-lane

### Performance assessment of PPP-AR with low-cost antennas

In this section, we analyze the PPP-AR positioning performance in terms of ambiguity resolution and coordinate accuracy domains. The positioning results are then referred to the quality of the PCC models of the employed low-cost antennas and their susceptibility to the multipath effect.

#### Ambiguity resolution performance

The ambiguity fixing rate (AFR) for a subset of independent ambiguities (Figs. 4 and 5) is calculated as the ratio of the number of resolved narrow-lane ambiguities to total ambiguities. Correctly fixed ambiguities of phase measurements improve the positioning accuracy. Therefore, high AFRs close to 100% confirm obtaining a reliable solution.

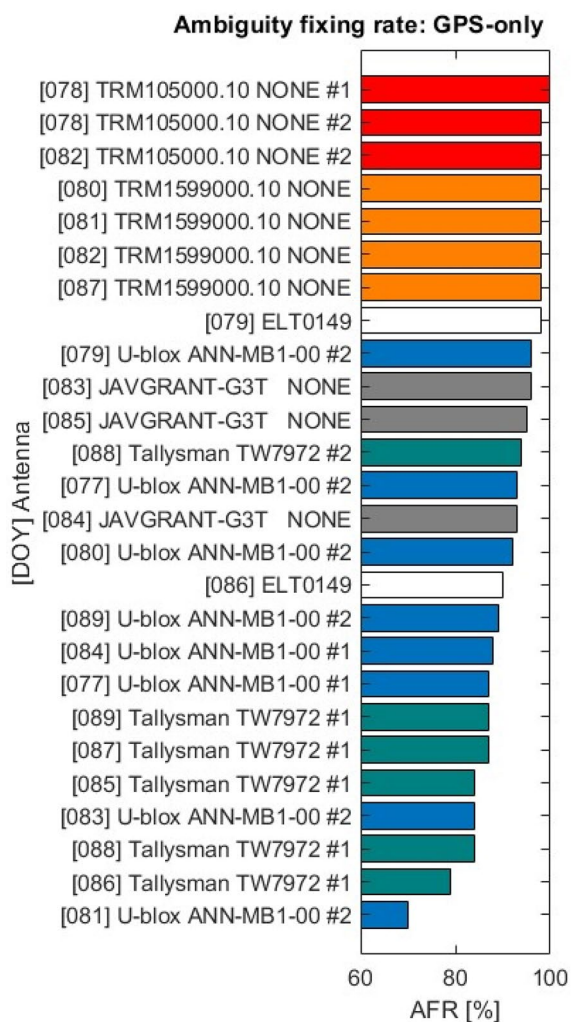


Fig. 4 Ambiguity fixing rates for GPS-only solution. The antenna units of the same model are given in the same color

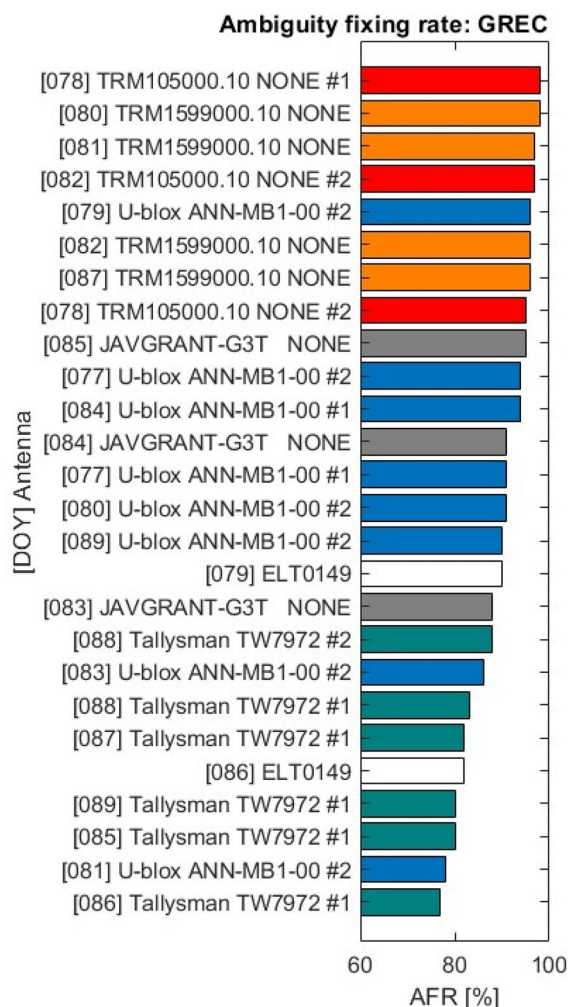


Fig. 5 Ambiguity fixing rates for GREC solution

It can be seen that the rates of fixed ambiguities drop significantly for low-cost antennas compared to geodetic ones, often below 90%. The AFRs obtained when using the TRM105000.10 and TRM159900.00 geodetic antennas are higher than 96%. AFR for the JAVGRANT-G3T antenna exceeds 91% for the GPS-only solution. For GREC, it is slightly lower, which we associate with the problems in recording Beidou signals described in the section on the number of recorded observations for individual antennas and GNSS systems. For low-cost antennas, most AFR values fit the 80–90% range. The lowest AFR values were obtained on March 22, 2022 (DOY 81), for the U-blox ANN-MB-00 antenna. Then, AFR equaled 70% and 78% for GPS-only and quadruple-system solutions, respectively. On March 27, 2022 (DOY 86) AFR for the Tallysman TW7972 equaled 79% and 77% for GPS-only and quadruple-system solutions, respectively. In comparison, on March 22, 2022, when using the TRM159900.00 antenna, the AFR reached 98% and 97%, respectively. When evaluating ambiguity resolution

performance, we discovered no advantage of the Tallysman TW7972 antenna having a PCC model from calibration over the other low-cost antennas. In order to check the effect of PCO/PCC corrections on AFR, we once again performed processing observations without using these corrections. Slightly fewer zero difference ambiguities were detected without corrections but ultimately the single-difference AFR was mostly the same. In the case of the Tallysman and geodetic-grade antennas neglecting PCC in the GREC solution, there were isolated instances of fixing one less narrow-lane ambiguity resulting in a 1% reduction in AFR. Therefore, it can be concluded that the lack of PCO/PCC corrections has a marginal effect on AFR, and the lower values of this parameter in our study are mainly due to the quality and design of the antennas.

## Static positioning performance

The results of static PPP positioning for the 16 h sessions are summarized in Table 5. Each column shows the coordinate bias of the east (E), north (N), and height (U) components computed for each day with respect to the benchmark position of two mounting points. The benchmark coordinates were obtained by means of a multi-constellation static solution based on the datasets collected 78 and 80 DOYs with the use of TRM105000.10 NONE and TRM159900.00 NONE choke-ring antennas and Trimble Alloy receiver. Such reference solutions are characterized by a high AFR and low standard deviation of the coordinates.

Deviations from the reference position for solutions obtained using choke-ring antennas are characterized by the smallest values, exceeding 5 mm for horizontal coordinates

**Table 5** Coordinate bias of PPP-AR solutions with respect to the benchmark position

DOY	Antenna	PCC model	Mounting point #1					
			G			GREC		
			E [mm]	N [mm]	U [mm]	E [mm]	N [mm]	U [mm]
077	U-blox ANN-MB-00 #1	U-blox PCO	-1.9	-4.3	-46.4	-3.8	-3.9	-41.1
078	TRM105000.10 NONE #1	IGS14_2196	-1.7	-0.9	-0.7	0.0	0.0	0.0
079	U-blox ANN-MB-00 #2	U-blox PCO	-9.9	-10.4	-36.0	-8.6	-8.8	-37.0
080	U-blox ANN-MB-00 #2	U-blox PCO	-9.3	-10.7	-34.0	-8.9	-8.0	-35.3
081	U-blox ANN-MB-00 #1	U-blox PCO	4.1	1.7	-35.8	3.6	-1.1	-36.2
082	TRM105000.10 NONE #1	IGS14_2196	-4.7	0.7	12.9	-5.4	0.9	12.9
083	U-blox ANN-MB-00 #2	U-blox PCO	-3.7	-6.4	-59.6	-5.8	-2.6	-42.1
084	U-blox ANN-MB-00 #1	U-blox PCO	-3.4	-5.0	-21.6	-2.6	-2.8	-17.6
085	Tallysman TW7972 #1	Tallysman	-10.0	-2.4	-25.5	-9.3	-1.8	-19.7
086	Tallysman TW7972 #1	Tallysman	-9.5	-3.1	-23.7	-6.9	-1.4	-22.3
087	Tallysman TW7972 #1	Tallysman	-7.6	-3.7	-16.0	-4.5	-1.8	-12.8
088	Tallysman TW7972 #1	Tallysman	-9.5	-2.2	-14.9	-6.0	-1.6	-14.7
089	Tallysman TW7972 #1	Tallysman	-6.7	-1.7	-17.3	-4.8	-0.9	-18.1
DOY	Antenna	PCC model	Mounting point #2					
			G			GREC		
			E [mm]	N [mm]	U [mm]	E [mm]	N [mm]	U [mm]
077	U-blox ANN-MB-00 #2	U-blox PCO	-3.0	-10.0	-26.7	-0.1	-10.4	-25.5
078	TRM105000.10 NONE #2	IGS14_2196	2.1	0.6	12.4	1.4	1.5	14.9
079	ELT0149	Zero	-18.7	7.0	-0.4	-17.3	6.3	-8.1
080	TRM159900.00 NONE	IGS14_2196	0.4	-1.6	2.6	0.0	0.0	0.0
081	TRM159900.00 NONE	IGS14_2196	-0.5	-0.5	4.2	-1.4	0.5	2.2
082	TRM159900.00 NONE	IGS14_2196	-1.4	-1.2	8.9	-2.5	0.0	8.3
083	JAVGRANT-G3T NONE	IGS14_2196	5.3	2.9	16.4	-2.3	2.0	33.4
084	JAVGRANT-G3T NONE	IGS14_2196	3.4	3.7	17.0	-2.7	2.6	32.8
085	JAVGRANT-G3T NONE	IGS14_2196	1.5	2.9	18.5	-4.2	0.3	33.0
086	ELT0149	Zero	-21.3	-10.7	-8.5	-18.1	-10.2	-19.7
087	TRM159900.00 NONE	IGS14_2196	1.8	-3.2	13.6	2.0	-2.5	15.7
088	Tallysman TW7972 #2	Tallysman	3.8	1.0	-13.3	2.8	1.0	-13.5
089	U-blox ANN-MB-00 #2	U-blox PCO	4.8	-12.9	-24.3	4.8	-11.6	-13.9



and 10 mm for height only in some individual cases. Slightly inferior accuracy but only with regard to height determination are the results of positioning with the JAVGRANT-G3T NONE geodetic antenna. For the GPS-only solution, the offset in height varies in the range of 15–20 mm. Interestingly, for the GREC solution, this value is as high as approximately 33 mm. We again attribute such an effect to the lack of information about the antenna PCC for signals from Galileo and BDS constellations for JAVGRANT-G3T. In this case, the antenna PCC for Galileo and BDS are adapted from the corresponding GPS signals, what could have caused the shift described above (Araszkiewicz and Kliszek 2020). In addition, the shift may have been influenced by difficulties in recording the Beidou signals described in Table 3 and the related text.

The results for the low-cost Tallysman TW7972 antenna, the only one of those tested with a phase center model, agree well with the reference position. For the horizontal components, the N value is slightly higher, up to 5–10 mm. The height deviation, on the other hand, exceeded 20 mm in some cases. As expected, including REC observations in the processing apparently reduced the difference between the received and reference positions. In the case of the second low-cost U-blox ANN-MB-00 antenna, a slightly larger offset for the horizontal components is apparent, sometimes exceeding 10 mm. However, the shift is significant for the vertical component, ranging from 20 mm to as much as nearly 60 mm. As expected, the results for the cheapest antenna in the list, ELT0149, are characterized by the highest horizontal shift of more than 20 mm for the E component.

### Kinematic positioning performance

Figure 6 and 7 give us the first impression of the kinematic positioning performance that may be achieved with the low-cost and high-grade antennas. The figures present a sample of time series of PPP-AR positioning errors for kinematic daily solutions. What transpires from the figure is that the geodetic antennas provide better stability of the position time series. The solutions obtained using low-cost antennas are characterized by less regularity and higher noise.

A more comprehensive analysis of the kinematic positioning performance with low-cost antennas is provided in Table 6, in which we show the positioning performance statistics of the kinematic PPP-AR kinematic solutions. The columns show the standard deviation values of the east, north, and height components. The values of the standard deviation clearly separate geodetic antennas from the low-cost ones. In the case of the GPS-only solution for low-cost antennas, almost all coordinate error standard deviations exceed 10 mm or 20 mm in the horizontal and vertical planes, respectively. The situation is significantly improved

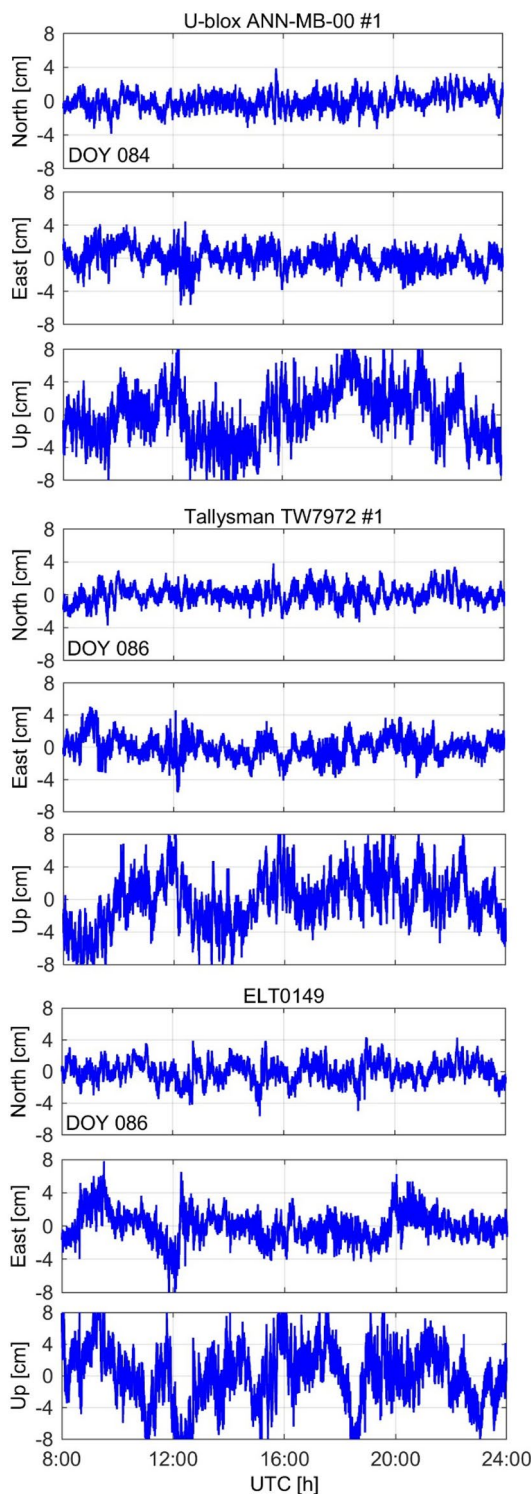
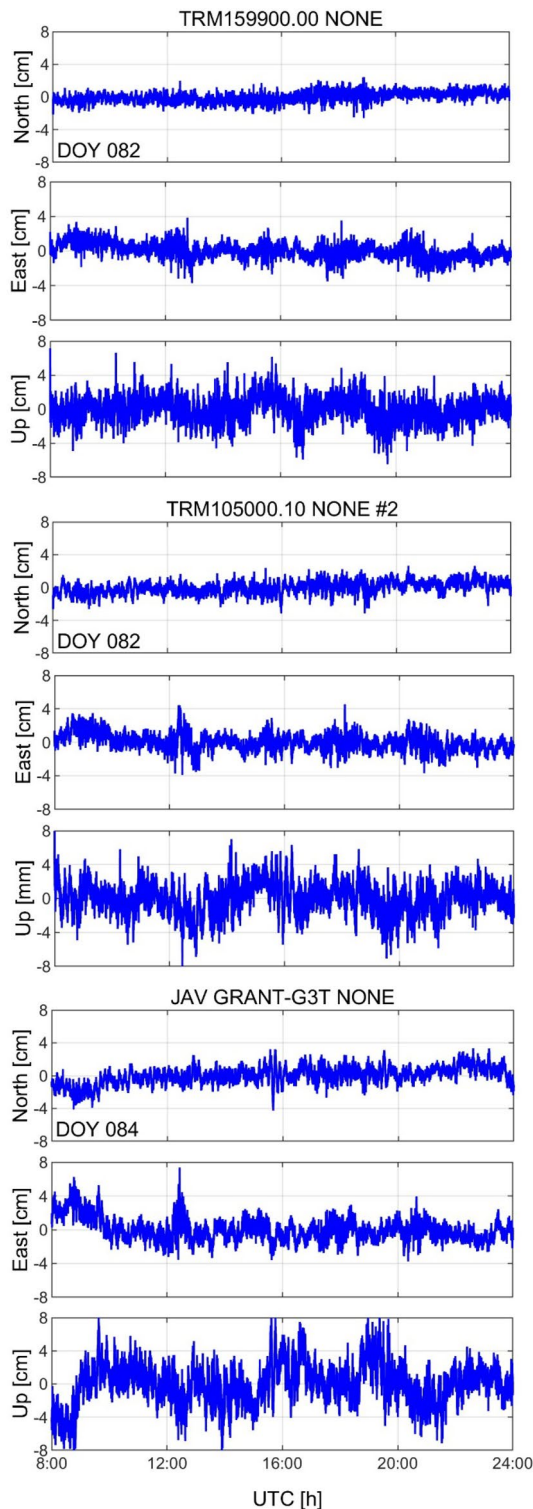


Fig. 6 Coordinate residuals time series of GPS-only PPP-AR kinematic solution for low-cost antennas

when including observations from all GNSS systems. In the case of mass-market antennas, almost all standard deviations of the horizontal components drop to a level below 10 mm.



**Fig. 7** Coordinate residuals time series of GPS-only PPP-AR kinematic solution for high-grade antennas

For the vertical component, when using Tallysman TW7972 or ELT0149 antennas, only a few STDs exceed the adopted 20 mm threshold.

The results also reveal the significant benefit of using multi-constellation signals on precision in the kinematic solution for all antennas, from 3% up to 58% and about 40% on average. Such an effect is obtained, although even if antenna phase center corrections are provided, they are available only for GPS and GLONASS constellations. Kinematic PPP-AR highlights the divergences between high-grade and low-cost equipment as low-budget antennas provided the solutions with at least 1.5 times higher coordinate standard deviation compared to geodetic antennas.

### A focus on the multipath impact

In Figs. 8 and 9, we show the time series of code (PR) and phase (CP) IF observation residuals and elevation angles for the representative GPS satellite PRN 26, for low-cost and reference TRM159900.00 antennas. The plot of CP residuals (Fig. 9) shows the repeatability of the plot shape for consecutive days from the processing using low-cost antennas, as well as greater fluctuation, which corresponds to lower positioning accuracy. Additionally, there are gaps in the recorded observations for the ELT0149 and U-blox ANN-MB-00 antennas. TRM159900.00, as expected, has the smallest residual variation. Conclusions from the analysis of PR residuals are similar, although the differences between Tallysman TW7972 and U-blox ANN-MB-00 and reference TRM159900.00 antenna are smaller than for CP residuals.

Figures 10 and 11 present the multipath for GPS L1 and L2 frequencies derived from CMC linear combination for the same data set. The plots confirm the presence of multipath effect at the site as well as the significant susceptibility of the low-cost antennas to the multipath for low-elevated satellites. Noticeably, the plot is heavily scattered for low elevation angles, particularly for the ELT0149 antenna. The results from the Tallysman TW7972 and the U-blox ANN-MB-00 are more similar to those from the TRM159900.00 antenna. However, a much larger fluctuation for higher elevation angles for the low-cost antennas can be seen. This regularity is even more evident in the case of the L2 frequency (Fig. 11). The source of the multipath is most likely the sloping roof with a wavy ceramic covering and the chimney on which the test beam is located. In our study, we tried to confirm this according to the methodology described by Teunissen and Montenbruck (2017), but the size of the roof, the slanted orientation, and the corrugated structure made it difficult to draw firm conclusions.

Tables 7 and 8 present the RMSs of MP from CMC linear combination for different frequencies for GPS and Galileo signals. The results confirm the predominance of high-grade antennas in terms of multipath susceptibility. In the case of the L1 GPS frequency, the differences in the RMS of MP values are small. All values are close to 0.3 m, slightly favoring Trimble professional antennas. For L2 GPS, the

**Table 6** Standard deviations of coordinate residuals from PPP-AR kinematic solutions

DOY	Antenna	PCC model	Mounting point #1					
			G			GREC		
			STD [mm]			STD [mm]		
			E	N	U	E	N	U
077	U-blox ANN-MB-00 #1	U-blox PCO	10.1	12.4	26.1	6.2	6.8	17.2
078	TRM105000.10 NONE #1	IGS14_2196	6.4	8.7	18.9	3.9	5.2	14.2
079	U-blox ANN-MB-00 #2	U-blox PCO	8.3	11.6	25.4	5.2	6.0	16.4
080	U-blox ANN-MB-00 #2	U-blox PCO	8.3	11.4	24.5	5.5	5.9	14.0
081	U-blox ANN-MB-00 #1	U-blox PCO	16.8	14.0	39.7	7.3	7.2	19.7
082	TRM105000.10 NONE #1	IGS14_2196	7.4	9.7	17.4	5.3	6.6	10.4
083	U-blox ANN-MB-00 #2	U-blox PCO	14.8	13.0	34.8	6.2	8.3	18.5
084	U-blox ANN-MB-00 #1	U-blox PCO	10.0	12.0	31.1	5.7	7.4	17.8
085	Tallysman TW7972 #1	Tallysman	11.7	12.3	29.0	6.9	7.0	23.7
086	Tallysman TW7972 #1	Tallysman	10.2	12.9	31.3	6.6	8.1	23.2
087	Tallysman TW7972 #1	Tallysman	11.8	12.8	32.3	7.9	9.0	15.8
088	Tallysman TW7972 #1	Tallysman	11.1	12.9	28.9	6.5	8.8	20.5
089	Tallysman TW7972 #1	Tallysman	10.6	13.2	32.2	6.2	7.1	16.8
DOY	Antenna	PCC model	Mounting point #2					
			G			GREC		
			STD [mm]			STD [mm]		
			E	N	U	E	N	U
077	U-blox ANN-MB-00 #2	U-blox PCO	9.5	11.8	24.9	6.2	6.5	18.3
078	TRM105000.10 NONE #2	IGS14_2196	7.7	9.1	21.2	4.2	5.2	13.7
079	ELT0149	Zero	11.0	18.4	27.1	7.0	8.1	21.4
080	TRM159900.00 NONE	IGS14_2196	5.3	6.9	12.4	4.1	4.2	9.9
081	TRM159900.00 NONE	IGS14_2196	5.4	7.4	11.9	4.1	4.9	7.3
082	TRM159900.00 NONE	IGS14_2196	6.0	8.6	13.7	4.7	6.4	8.3
083	JAVGRANT-G3T NONE	IGS14_2196	9.6	10.7	23.2	5.4	6.8	15.4
084	JAVGRANT-G3T NONE	IGS14_2196	10.5	13.1	24.1	5.3	7.3	20.4
085	JAVGRANT-G3T NONE	IGS14_2196	8.5	13.0	21.4	5.9	7.2	15.3
086	ELT0149	Zero	12.8	17.5	37.4	9.0	12.0	21.1
087	TRM159900.00 NONE	IGS14_2196	5.2	7.2	13.1	3.5	5.0	9.4
088	Tallysman TW7972 #2	Tallysman	10.2	13.1	24.3	7.1	8.9	23.6
089	U-blox ANN-MB-00 #2	U-blox PCO	11.4	13.7	31.5	6.4	7.4	19.0
Antenna	PCC model	Mean values						
		G			GREC			
		STD [mm]			STD [mm]			
		E	N	U	E	N	U	
U-blox ANN-MB-00	U-blox PCO	11.2	12.5	29.8	6.1	6.9	17.6	
Tallysman TW7972	Tallysman	10.9	12.9	29.7	6.9	8.2	20.6	
ELT0149	Zero	11.9	18.0	32.3	8.0	10.1	21.3	
TRM159900.00 NONE	IGS14_2196	5.5	7.5	12.8	4.1	5.1	8.7	
TRM105000.10 NONE	IGS14_2196	7.2	9.2	19.2	4.5	5.7	12.8	
JAVGRANT-G3T NONE	IGS14_2196	9.5	12.3	22.9	5.5	7.1	17.0	

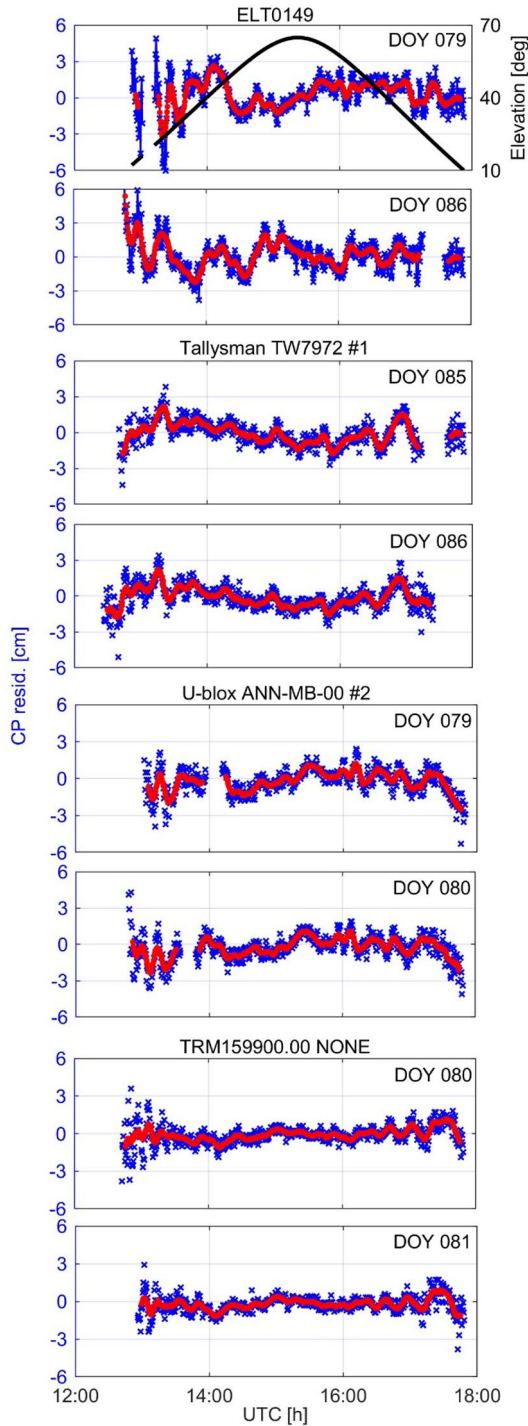


**Fig. 8** Carrier phase IF residuals and elevation angle for GPS PRN 26 satellite for three tested low-cost antennas and high-grade TRM159900.00 one (bottom)

differences in RMS of MP values are already much more noticeable—for U-blox ANN-MB-00 and ELT0149 antennas, the RMS of MP exceeds 0.60 m in some cases, and for Tallysman TW7972, it is slightly lower, amounting to 0.49–0.53 m. At the same time, these values for professional

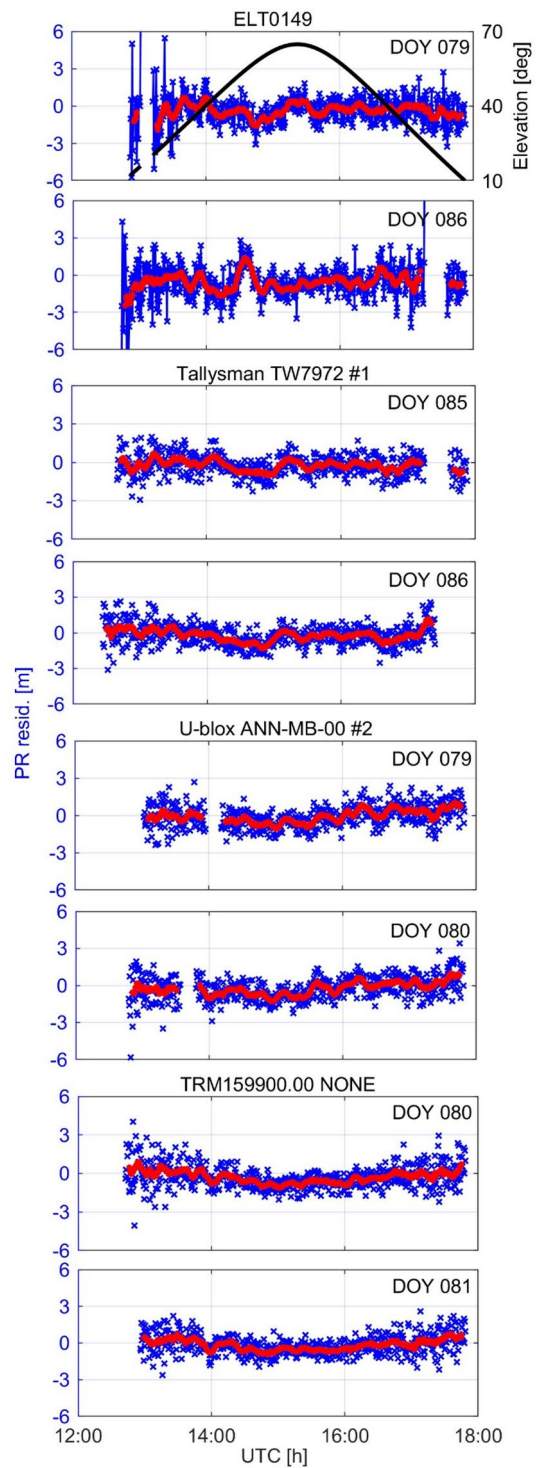


**Fig. 9** Pseudorange IF residuals and elevation angle for GPS PRN 26 satellite for three tested low-cost antennas and high-grade TRM159900.00 one (bottom)

antennas range from 0.32–0.38 m for Trimble antennas L2 GPS and 0.44 m for JAVGRANT-G3T L2 GPS. We also

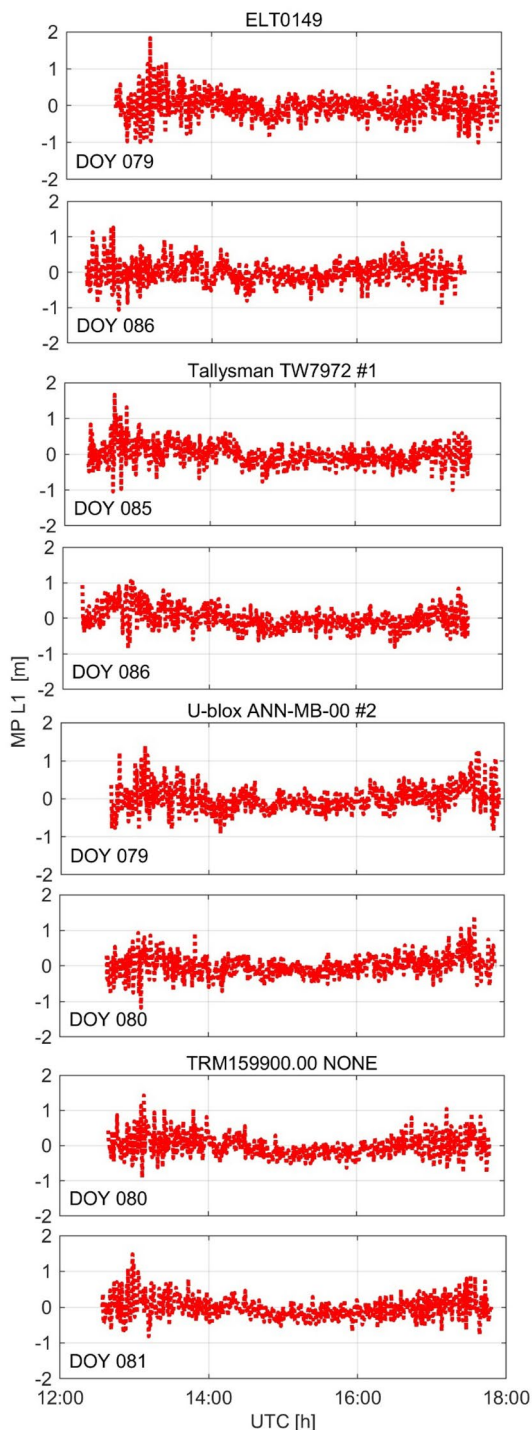


**Fig. 10** MP of L1 from CMC linear combination for GPS PRN 26 satellite for the low-cost antennas (top three) and TRM159900.00 (bottom)

note that the results obtained for different units of the same antenna type for consecutive days agree well.

For Galileo E1 frequency, the results are similar to those of GPS L1. The exceptions are the results for the

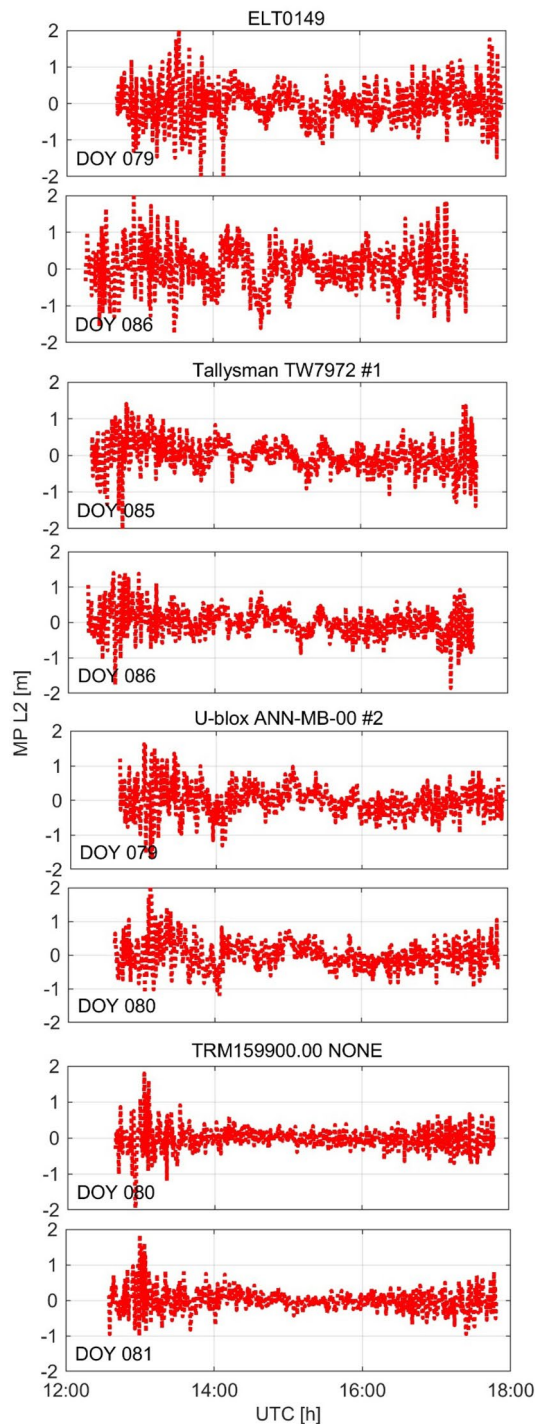


**Fig. 11** MP of L2 from CMC linear combination for GPS PRN 26 satellite for the low-cost antennas (top three) and TRM159900.00 (bottom)

TRM159900.00 reference antenna, for which the RMSs of MP values are between 0.20 and 0.22 m. Even better results, below the 0.2 m value, were obtained for this antenna at E5a frequencies. Values close to 0.30 m characterized the E5a RMS of MP values for the TRM105000.10 antenna, 0.35 m

**Table 7** RMS of MP from CMC for different frequencies of GPS

DOY	Antenna	RMS of MP for frequency [m]		Antenna	RMS of MP for frequency [m]	
		Mounting point #1	L1 L2		Mounting point #2	L1 L2
077	U-blox ANN-MB-00 #1	0.33	0.49	U-blox ANN-MB-00 #2	0.34	0.56
078	TRM105000.10 NONE #1	0.28	0.37	TRM105000.10 NONE #2	0.30	0.38
079	U-blox ANN-MB-00 #2	0.32	0.50	ELT0149	0.33	0.60
080	U-blox ANN-MB-00 #2	0.31	0.50	TRM159900.00 NONE	0.30	0.32
081	U-blox ANN-MB-00 #1	0.32	0.58	TRM159900.00 NONE	0.29	0.32
082	TRM105000.10 NONE #1	0.28	0.37	TRM159900.00 NONE	0.29	0.32
083	U-blox ANN-MB-00 #2	0.32	0.63	JAVGRANT-G3T NONE	0.31	0.44
084	U-blox ANN-MB-00 #1	0.33	0.51	JAVGRANT-G3T NONE	0.31	0.44
085	Tallysman TW7972 #1	0.31	0.49	JAVGRANT-G3T NONE	0.31	0.44
086	Tallysman TW7972 #1	0.31	0.49	ELT0149	0.35	0.64
087	Tallysman TW7972 #1	0.31	0.49	TRM159900.00 NONE	0.30	0.32
088	Tallysman TW7972 #1	0.31	0.49	Tallysman TW7972 #2	0.34	0.53
089	Tallysman TW7972 #1	0.31	0.49	U-blox ANN-MB-00 #2	0.34	0.63

**Table 8** RMS of MP from CMC for different frequencies of Galileo

DOY	Antenna	RMS of MP for frequency [m]		Antenna	RMS of MP for frequency [m]		
		Mounting point #1	E1		E5a	Mounting point #2	E1 E5a
077	U-blox ANN-MB-00 #1	0.32		0.40	U-blox ANN-MB-00 #2	0.33	0.44
078	TRM105000.10 NONE #1	0.28		0.27	TRM105000.10 NONE #2	0.29	0.30
079	U-blox ANN-MB-00 #2	0.31		0.41	ELT0149	0.34	0.50
080	U-blox ANN-MB-00 #2	0.32		0.43	TRM159900.00 NONE	0.22	0.19
081	U-blox ANN-MB-00 #1	0.33		0.45	TRM159900.00 NONE	0.20	0.18
082	TRM105000.10 NONE #1	0.27		0.27	TRM159900.00 NONE	0.21	0.19
083	U-blox ANN-MB-00 #2	0.33		0.50	JAVGRANT-G3T NONE	0.31	0.35
084	U-blox ANN-MB-00 #1	0.33		0.42	JAVGRANT-G3T NONE	0.29	0.34
085	Tallysman TW7972 #1	0.34		0.44	JAVGRANT-G3T NONE	0.32	0.37
086	Tallysman TW7972 #1	0.32		0.42	ELT0149	0.39	0.54
087	Tallysman TW7972 #1	0.33		0.43	TRM159900.00 NONE	0.20	0.18
088	Tallysman TW7972 #1	0.33		0.43	Tallysman TW7972 #2	0.34	0.52
089	Tallysman TW7972 #1	0.32		0.43	U-blox ANN-MB-00 #2	0.35	0.48

for JAVGRANT-G3T, and among the low-cost antennas 0.4–0.5 m for U-blox ANN-MB-00 and Tallysman TW7972 and above 0.5 m for ELT0149. As a result, the RMSs of MP for low-cost antennas are often more than double those for Trimble choke-ring antenna.

Analyzing the results for low-cost antennas only, it can be concluded that the ELT0149 antenna is the most susceptible to MP among the tested ones. The best results among the low-cost antennas are achieved for the Tallysman TW7972 antenna, which is reflected in the lowest RMS of MP values, although they are only marginally better than U-blox ANN-MB-00. Compared to professional high-grade antennas, the

RMSs of MP for low-cost ones are higher, from a few percent to twice, depending on the model and signal.

### Summary

In this study, we assessed the performance of PPP-AR with low-cost antennas, focusing on the impacts of multipath and receiver antenna phase center corrections. We employed three low-cost antenna models of various grades and three professional geodetic ones, characterized by different

completeness of the information on their PCO and PCV and expected susceptibility to the multipath effect.

We first analyzed AFR, which dropped significantly, often below 90%, when a low-cost antenna was used in the processing. In contrast, the AFR parameter was close to 100% for the employed professional antennas. These parameter values generally dropped even more when multi-constellation observations were used instead of GPS-only, which we attribute to the lack of receiver antenna phase center correction models for other constellations. When evaluating ambiguity resolution performance, there was no advantage of the Tallysman TW7972 antenna having a PCC model from calibration over the other low-cost antennas.

Static GPS PPP-AR for the low-cost Tallysman TW7972 antenna, which has a PCC from calibration, provided a solution with mean coordinate residuals below 10 mm and 4 mm for the N and E components, respectively. In the case of the uncalibrated low-cost U-blox ANN-MB-00 antenna, we experienced significantly poorer coordinate accuracy for the E component, for which the difference between the benchmark and determined position exceeded 10 mm. As expected, the worst performance was that of the cheapest antenna—ELT0149, which is not supported by the PCC model. In this case, the mean coordinate residuals were close to 20 mm and about 10 mm, for N and E components, respectively. In the case of height determination, the differences are much higher, ranging from a few millimeters to as much as 60 mm, mainly fluctuating around 20–40 mm.

Coordinate standard deviations for time series of kinematic solutions highlighted the differences in performance between high-grade and low-cost antennas. In the case of the GPS-only solution for the latter antennas, almost all standard deviations exceeded 10 mm for horizontal coordinates and 20 mm for height. Despite lower AFR values, the significant effect on improving precision in the kinematic solution was driven by applying multi-constellation signals. This is due to the much higher number of observations in a multi-GNSS solution, which reduces the impact of AFR on positioning accuracy. For all antennas, the standard deviation of position determination improved from 3% to as much as 58%, about 40% on average. However, low-budget antennas were still characterized by 1.5 to more than two times higher standard deviation values for all components than geodetic antennas. The worst results for this analysis were those obtained from the ELT0149 antenna without PCC from calibration.

The multipath analyses explain poorer positioning results for low-cost antennas compared to high-grade ones. The investigations showed significant differences in results depending on the signal. Although slightly higher for low-cost antennas, the RMSs of MP values for GPS L1 and Galileo E1 signals were similar. The situation was much worse for GPS L2 and Galileo E5a signals. Overall, it can be concluded that the RMSs of MP values for low-cost antennas

are higher, ranging from a few percent to as much as two times the value of RMS of MP for professional antennas, depending on the model and signal analyzed. Such outcomes were also confirmed by the nature of pseudorange and carrier phase residuals given as a function of the elevation angle of the satellites. Such values clearly showed that for elevation angles below 30 degrees, the observation residuals were much more scattered for low-cost antennas than for geodetic ones. Moreover, the multipath analysis revealed a noticeable advantage of the Tallysman TW7972 antenna having PCC from calibration over other low-cost antennas, especially for ELT0149, which has no such corrections. In both analyses, MP and observation residuals exhibited a slight advantage of the Tallysman TW7972 antenna having PCC from calibration over other U-blox ANN-MB-00. The weakest performing antenna was again ELT0149.

We conclude that when using low-cost antennas for precise geodetic applications, one should expect at least a two-fold decrease in positioning accuracy. To some extent, such an effect may be overcome when using signals from multiple satellite systems. However, it should be noted that this accuracy may drop even further in a multipath environment due to the susceptibility of low-cost antennas to this effect. We also report noticeable differences in positioning performance with different low-cost antennas that may be attributed to the completeness of the PCC models and antenna susceptibility to the multipath effect.

**Acknowledgements** This study was supported by the project “Innovative precise monitoring system based on integration of low-cost GNSS and IMU MEMS sensors” POIR 01.01.01-00-0753/21, co-financed by the European Regional Development Fund within the Sub-measure 1.1.1 of the Smart Growth Operational Program 2014–2020. We would like to express our great appreciation for GNSS products and the PRIDE PPP-AR software provided by Wuhan University.

**Author contributions** G.K. performed the computations. K.D. prepared observational data and figures. All authors contributed to analyzing and discussing the results, writing, and reviewing the manuscript.

**Funding** The authors have not disclosed any funding.

**Data availability** The GNSS observational data can be made available by contacting the authors upon request.

## Declarations

**Competing interests** The authors declare no competing interests.

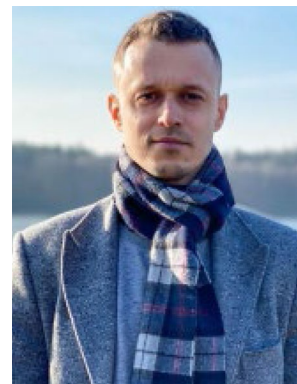
**Open Access** This article is licensed under a Creative Commons Attribution 4.0 International License, which permits use, sharing, adaptation, distribution and reproduction in any medium or format, as long as you give appropriate credit to the original author(s) and the source, provide a link to the Creative Commons licence, and indicate if changes were made. The images or other third party material in this article are included in the article’s Creative Commons licence, unless indicated otherwise in a credit line to the material. If material is not included in the article’s Creative Commons licence and your intended use is not

permitted by statutory regulation or exceeds the permitted use, you will need to obtain permission directly from the copyright holder. To view a copy of this licence, visit <http://creativecommons.org/licenses/by/4.0/>.

## References

- Araszkiewicz A, Kiliszek D (2020) Impact of using GPS L2 receiver antenna corrections for the galileo E5a frequency on position estimates. *Sensors* 20(19):5536. <https://doi.org/10.3390/s20195536>
- Bhuiyan M, Lohan E (2010) Advanced multipath mitigation techniques for satellite-based positioning applications. *Int J Navig Obs*. <https://doi.org/10.1155/2010/412393>
- Biagi L, Grec F, Negretti M (2016) Low-cost GNSS receivers for local monitoring: experimental simulation, and analysis of displacements. *Sensors*. <https://doi.org/10.3390/s16122140>
- Darugna F, Wübbena JB, Wübbena G, Schmitz M, Schön S, Warneke A (2020) Impact of robot antenna calibration on dual-frequency smartphone-based high-accuracy positioning: a case study using the Huawei Mate20X. *GPS Solutions*. <https://doi.org/10.1007/s10291-020-01048-0>
- Dilßner F, Seeber G, Wübbena G, Schmitz M (2008) Impact of near-field effects on the GNSS position solution. Proc. ION GNSS 2008, Savannah International Convention Center, Savannah, Georgia, USA, September 16–19, 872–884
- Garrido-Carretero M, de Lacy-Pérez Los Cobos M, Borque-Arancón M, Ruiz-Armenteros A, Moreno-Guerrero R, Gil-Cruz A (2019) Low-cost GNSS receiver in RTK positioning under the standard ISO-17123-8: a feasible option in geomatics. *Meas J Int Meas Confed*. <https://doi.org/10.1016/j.measurement.2019.01.045>
- Ge L, Han S, Rizos C (2000) Multipath mitigation of continuous GPS measurements using an adaptive filter. *GPS Solutions*. <https://doi.org/10.1007/PL00012838>
- Geng J, Chen X, Pan Y et al (2019) PRIDE PPP-AR: an open-source software for GPS PPP ambiguity resolution. *GPS Solut* 23:91. <https://doi.org/10.1007/s10291-019-0888-1>
- Görres B, Campbell J, Becker M, Siemes M (2006) Absolute calibration of GPS antennas: laboratory results and comparison with field and robot techniques. *GPS Solutions*. <https://doi.org/10.1007/s10291-005-0015-3>
- Guerova G et al (2016) Review of the state of the art and future prospects of the ground-based GNSS meteorology in europe. *Atmos Meas Tech* 9(11):5385–5406
- Guo J, Xu X, Zhao Q et al (2016) Precise orbit determination for quad-constellation satellites at Wuhan University: strategy, result validation, and comparison. *J Geodesy* 90:143–159. <https://doi.org/10.1007/s00190-015-0862-9>
- Hamza V, Stopar B, Ambrožič T, Sterle O (2021) Performance evaluation of low-cost multi-frequency gnss receivers and antennas for displacement detection. *Appl Sci*. <https://doi.org/10.3390/app11146666>
- Hohensinn R, Stauffer R, Glaner MF, Herrera Pinzón ID, Vuadens E, Rossi Y, Clinton J, Rothacher M (2022) Low-cost GNSS and real-time PPP: assessing the precision of the u-blox ZED-F9P for kinematic monitoring applications. *Remote Sens* 14(20):5100. <https://doi.org/10.3390/rs14205100>
- Hunegnaw A, Teferle NF (2022) Evaluation of the multipath environment using electromagnetic-absorbing materials at continuous GNSS stations. *Sensors*. <https://doi.org/10.3390/s22093384>
- Jackson J, Davis B, Gebre-Egziabher D (2018) A performance assessment of low-cost RTK GNSS receivers. Proc. IEEE/ION 2018 position, location and navigation symposium (PLANS), monterey, CA, USA, 642–649. <https://doi.org/10.1109/PLANS.2018.8373438>
- Moradi, R (2014) Carrier multipath mitigation in linear combinations of Global Navigation Satellite Systems measurements. Doctor Thesis, Centre for Transport Studies, Department of Civil and Environmental Engineering, Imperial College London. London, United Kingdom
- Parkinson, B., Spilker, J. (1996). Global positioning system: theory and applications, Vol. I, progress in astronautics and aeronautics. Washington DC, American Institute of Aeronautics and Astronautics
- Paziewski J (2022) Multi-constellation single-frequency ionospheric-free precise point positioning with low-cost receivers. *GPS Solutions*. <https://doi.org/10.1007/s10291-021-01209-9>
- Paziewski J, Sieradzki R, Baryla R (2019) Detection of structural vibration with high-rate precise point positioning: case study results based on 100 Hz multi-GNSS observables and shake-table simulation. *Sensors* 19:4832. <https://doi.org/10.3390/s19224832>
- Rougerie S, Carrié G, Vincent F, Ries L, Monnerat M (2012) A new multipath mitigation method for GNSS receivers based on an antenna array. *Int J Navig Obs*. <https://doi.org/10.1155/2012/804732>
- Teunissen PJG, Montenbruck O (2017) Springer handbook of global navigation satellite systems. Springer, Cham, Switzerland. <https://doi.org/10.1007/978-3-319-42928-1>
- Vázquez B, Grejner Brzeziska D (2012) A case of study for pseudorange multipath estimation and analysis: TAMDEF GPS network. *Geofísica Internacional* 51(1):63–72. <https://doi.org/10.22201/igeof.00167169p.2012.51.1.146>
- Volk CM, Levine J (1994) Analytical estimation of carrier multipath bias on GPS position measurements. Boulder, CO., USA
- Wübbena G, Schmitz M, Boettcher G, Schumann C (2006) Absolute GNSS antenna calibration with a robot: repeatability of phase variations, calibration of GLONASS and determination of carrier-to-noise pattern. proceedings of the IGS workshop
- Xue C, Psimoulis P, Zhang Q, Meng X (2021) Analysis of the performance of closely spaced low-cost multi-GNSS receivers. *Appl Geomat*. <https://doi.org/10.1007/s12518-021-00361-8>

**Publisher's Note** Springer Nature remains neutral with regard to jurisdictional claims in published maps and institutional affiliations.

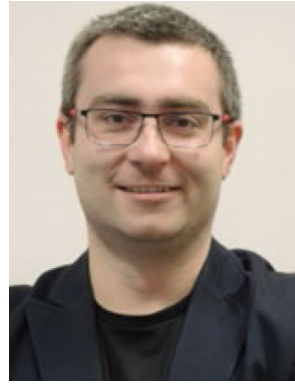


**Grzegorz Krzan** Received his PhD in Satellite Geodesy from the University of Warmia and Mazury in Olsztyn in 2018. His current research involves Precise Point Positioning, GNSS signals interference phenomena, and GNSS antenna phase center variations modeling





**Karol Dawidowicz** Received his Ph.D. in Satellite Geodesy from the University of Warmia and Mazury in Olsztyn in 2001. His research interests cover GNSS leveling, GNSS antenna phase center variations modeling, and Precise Point Positioning. He is a member of the Advanced Methods of GNSS Data Processing Group



**Jacek Paziewski** Is an associate professor at the University of Warmia and Mazury in Olsztyn. His research interests include developing multi-GNSS positioning algorithms, modeling the ionospheric delays, smartphone and low-cost receiver positioning, and high-rate data processing